



## Preparation of Poly(3-hydroxybutyrate-*b*- $\epsilon$ -caprolactone) by Reactive Extrusion and Production of Electrospun Fibrous Mats

Katia Y. Sakaguti<sup>1b</sup>\*<sup>a</sup> and Shu H. Wang<sup>1b</sup><sup>a</sup>

<sup>a</sup>Departamento de Engenharia Metalúrgica e de Materiais, Escola Politécnica, Universidade de São Paulo, Av. Professor Mello Moraes, 2463, 05508-030 São Paulo-SP, Brazil

Poly(3-hydroxybutyrate) (PHB) has been proposed to be a potential candidate to be used as biomaterial. However, its poor processability, high brittleness and rigidity have limited its applicability. Transesterification reactions with poly( $\epsilon$ -caprolactone) (PCL), one of the most promising biomedical materials, emerge as an attractive alternative to improve its mechanical properties. In this work, poly(3-hydroxybutyrate-*b*- $\epsilon$ -caprolactone) (PHB-*b*-PCL) was prepared straightforwardly by transesterification of the parent homopolymers by reactive extrusion in the presence of stannous octanoate. After purification by solvent fractionation, PHB-*b*-PCL was characterized by differential scanning calorimetry (DSC), Fourier transform infrared spectroscopy (FTIR) and nuclear magnetic resonance spectroscopy of carbon (<sup>13</sup>C NMR) and hydrogen (<sup>1</sup>H NMR) and, subsequently, submitted to electrospinning. The results indicate that PHB was modified, showing lower crystallinity as compared to the original homopolymers. The electrospun mats are tough and flexible and analysis by scanning electron microscopy indicates the formation of uniformly smooth morphology with average fiber diameter of 900-1200 nm and voids in the range between a few microns up to a few tens of microns, suitable for cell diffusion in biomedical applications.

**Keywords:** biodegradable polymers, PHB-*b*-PCL, electrospinning, biomaterials

### Introduction

Poly(3-hydroxybutyrate) (PHB) has been presented as one of the most environmentally friendly polymers to substitute non-biodegradable polymers in commercial applications. PHB has an excellent biocompatibility and controlled biodegradation,<sup>1</sup> and has been demonstrated to be a good candidate for tissue engineering and wound dressing, especially when used as electrospun ultrafine fibers mats.<sup>2-5</sup>

PHB belongs to the class of polyhydroxyalkanoates (PHAs), natural aliphatic polyesters produced by bacteria fermentation. PHB can be obtained from renewable sources, such as sugarcane, one of the most important energy crops in tropical countries, such as Brazil and India.<sup>6</sup> Sugarcane can be a key crop for PHB production because it has a very large biomass.<sup>7,8</sup> In addition, it is possible to obtain PHB from bagasse, a waste product of the sugar and alcohol industry,<sup>9,10</sup> minimizing the high amounts of residue produced.

The PHB practical implementation as biomaterial is restricted due to some limitations, such as poor processability and high brittleness and stiffness due to its high degree of crystallinity,<sup>11-13</sup> a consequence of its perfect stereoregularity and high purity resulting from its bacterial production.<sup>14</sup> To overcome its restrictions, PHB is often blended or copolymerized with other polymers, such as poly( $\epsilon$ -caprolactone) (PCL), synthetic polyester, also biodegradable, biocompatible and widely used in biomedical applications.<sup>12,15,16</sup> In contrast to PHB, PCL possesses good mechanical properties<sup>16,17</sup> and can be easily processed at relatively low temperatures.<sup>15</sup> Transesterification of PHB and other homopolyesters is an alternative method to synthesize copolyesters in a one-step catalytic synthesis.<sup>18</sup>

Kim and Woo<sup>19</sup> synthesized PHB/PCL copolyesters by transesterification in solution phase in the presence of dibutyltin oxide as catalyst, in order to increase the miscibility in the blends of PHB and PCL. Impallomeni *et al.*<sup>20</sup> synthesized the copolymer poly(3-hydroxybutyrate-*co*- $\epsilon$ -caprolactone) (PHB-*co*-PCL) by transesterification of homopolymers, conducted in solution, in the presence

\*e-mail: katysakaguti@usp.br

of 4-toluenesulfonic acid. Chen *et al.*<sup>18</sup> also synthesized it by transesterification in liquid phase in the presence of stannous octanoate.

One efficient method to process biodegradable polymers is by reactive extrusion, in which melt extrusion and chemical reaction occur simultaneously. Reactive extrusion offers some advantages such as simplicity, cost effectiveness, control of the residence times, and it does not require solvents.<sup>21,22</sup>

By copolymerizing PHB with PCL, a biodegradable and biocompatible material with enhanced mechanical properties and processability should be expected, increasing PHB applicability in tissue engineering. Electrospinning was chosen in this study since it is an excellent and simple method to produce micron/submicron diameter fiber mats and membranes to be employed as scaffolds.<sup>13,23</sup> So far, we have found no literature on PHB-*co*-PCL fibrous mats prepared by electrospinning.

In this work, transesterification of PHB and PCL was carried out by reactive extrusion processing in the presence of stannous octanoate as catalyst in order to synthesize poly(3-hydroxybutyrate-*block*- $\epsilon$ -caprolactone) (PHB-*b*-PCL). After purification by selective fractionation, the copolymer was characterized by differential scanning calorimetry (DSC), Fourier transform infrared spectroscopy (FTIR), carbon-13 and hydrogen nuclear magnetic resonance spectroscopy (<sup>13</sup>C and <sup>1</sup>H NMR) and solubility tests. Furthermore, this research explored the possibility of producing mats comprised by PHB-*b*-PCL nanofibers through electrospinning, suitable for tissue engineering applications.

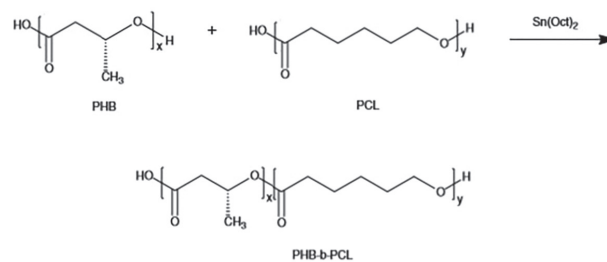
## Experimental

### Materials

Bacterial poly(3-hydroxybutyrate) (PHB), obtained by sugarcane, was supplied by PHB Industrial S.A. (Serrana, Brazil). Its weight-average molecular mass (Mw) determined by gel permeation chromatograph (GPC) was 266,700 g mol<sup>-1</sup>. Poly( $\epsilon$ -caprolactone) (PCL), with a reported number-average molecular mass (Mn) of 80,000 g mol<sup>-1</sup>, and stannous octanoate [Sn(Oct)<sub>2</sub>] were purchased from Sigma-Aldrich (St. Louis, USA). Chloroform (CHCl<sub>3</sub>), methanol (MeOH) and dichloromethane (DCM) were supplied by CAAL (São Paulo, Brazil). Tetrahydrofuran (THF) and 1,2-dichloroethane (DCE) were provided by Synth (Diadema, Brazil) and Merck (Darmstadt, Germany), respectively. All the reagents were used as received without any further treatment.

### Synthesis of PHB-*b*-PCL by reactive extrusion and purification

Initially, a blend of PHB and PCL at molar ratio 1:1 was prepared and dried under vacuum at 60 °C for 24 h. Under nitrogen atmosphere, 5 wt.% of Sn(Oct)<sub>2</sub> was added to the mixture. Scheme 1 shows the reaction mechanism. In a glove box, the components were mixed on a heating plate until a visually homogeneous molten mixture was formed. The mixture was cooled and reduced to small pieces, then the material was gradually placed in the cooled hopper of a Laboratory Mixing Extruder (LME, Dynisco), for reactive extrusion processing. The extrusion was carried out under nitrogen flow and the processing temperatures were set at 165 °C (mixing chamber) and 165 °C (extrusion die). To remove the starting homopolymers and the catalyst, the extruded material was dissolved in dichloromethane and kept in an ultrasonic bath at 38 °C for 3 h, then filtered, for unreacted PHB separation, and the remaining filtrate precipitated in methanol under magnetic stirring. The precipitate was dried in a vacuum oven and further fractionated by dissolution in dichloromethane and precipitation in methanol to remove the unreacted PCL that remained soluble in the solvent mixture. PHB-*b*-PCL was recovered by filtration and a yellowish-white powder was obtained after drying in a vacuum oven (yield = 32%, Mn = 19,230 and Mw = 28,230 g mol<sup>-1</sup>).



**Scheme 1.** Synthesis reaction of PHB-*b*-PCL copolymer.

### Characterization of PHB-*b*-PCL

Solubility tests were carried out by using different solvents (CHCl<sub>3</sub>, MeOH, DCM, THF and DCE). About 1.0 mg of polymer was introduced into a test tube containing 1.0 mL of each solvent tested. The tubes were immersed in a bath thermostated at 40 °C for 5 to 10 min and solubility was established by visual examination; the results were analyzed taking into account the Hansen solubility parameters of the components. Fourier transform infrared (FTIR) spectra were obtained using the Thermo Scientific Nicolet iS50 spectrophotometer in the attenuated

total reflectance (ATR) mode with a ZnSe crystal. The spectra were collected at room temperature with a scan number of 16 and resolution of  $4\text{ cm}^{-1}$ . Nuclear magnetic resonance spectroscopy ( $^{13}\text{C}$  and  $^1\text{H}$  NMR) was carried out on a Bruker AIII 500 MHz spectrometer. The NMR spectra were recorded at  $23\text{ }^\circ\text{C}$  in chloroform-*d* ( $\text{CDCl}_3$ ) solution. Thermal analysis was carried out by using a Netzsch DSC 200F3 differential scanning calorimeter. The samples were cooled from room temperature to  $-120\text{ }^\circ\text{C}$ , and then maintained at  $-120\text{ }^\circ\text{C}$  for 5 min before heating to  $200\text{ }^\circ\text{C}$  at a rate of  $10\text{ }^\circ\text{C min}^{-1}$ . A second heating cycle was followed, after cooling to  $-120\text{ }^\circ\text{C}$ , a final heating to  $200\text{ }^\circ\text{C}$  at a rate of  $10\text{ }^\circ\text{C min}^{-1}$  was recorded.

### Electrospinning of PHB-*b*-PCL

Polymer solutions for electrospinning were prepared by dissolving a pre-established amount of PHB-*b*-PCL in chloroform in order to reach concentrations of 20 and 25 wt.%. The electrospinning system is comprised by an injection pump (Nikkiso PSK-01, Japan), equipped with a 20 mL plastic syringe connected to a stainless steel needle (22 Gauge) without tip, a high voltage power source (Faíscas, Brazil) and a grounded collector covered with an aluminum foil placed vertically. The voltage was applied between the needle, ejection point, and the collector plate covered by aluminum foil and was set at 12 kV; the pumping rate was varied from  $1.0$  to  $1.2\text{ mL h}^{-1}$  and the working distance (distance between the tip of the needle and the collector) was kept constant at 15 cm.

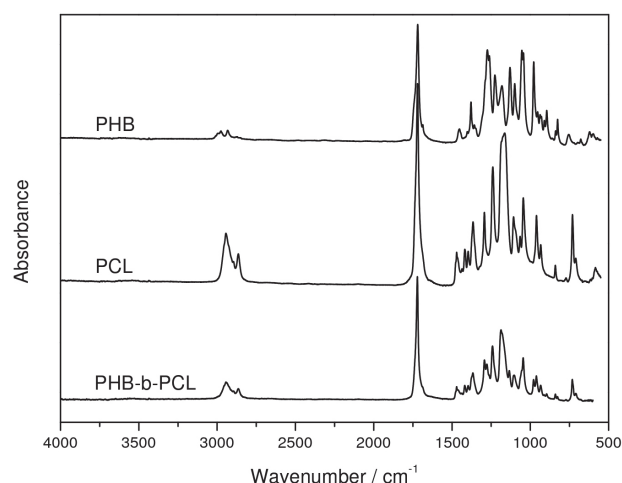
### Scanning electron microscopy of the electrospun mats

The electrospun mats were analyzed by scanning electron microscopy (SEM, FEI Inspect F50 FEG) in order to verify the formation of polymer fibers and to observe the morphology. Fiber diameters were statistically calculated using ImageJ software and DiameterJ plugin.<sup>24</sup>

## Results and Discussion

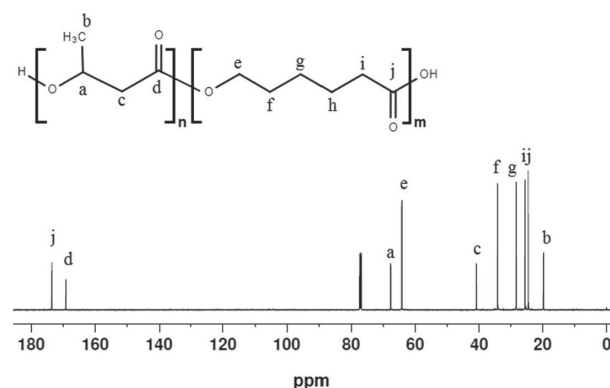
The FTIR technique is an efficient tool to obtain information on polymer copolymerization, such as interactions detection and creation of new chemical bonds. Figure 1 illustrates FTIR spectra of PHB, PCL and PHB-*b*-PCL. The bands for PHB and PCL present chemical similarity. Characteristic bands for PHB and PCL were at  $1715\text{ cm}^{-1}$  assigned to the stretching of C=O bond, whereas a series of intense bands of axial deformation in the region of  $1100$  to  $1300\text{ cm}^{-1}$  correspond to C–O bonds of the ester group. In the PHB spectrum, the peak observed

at about  $1380\text{ cm}^{-1}$  is related to the symmetrical wagging of  $\text{CH}_3$  group, the same observed in the PHB-*b*-PCL spectrum. In the PCL spectrum, a band of strong intensity observed at  $730\text{ cm}^{-1}$  is related to CH rocking vibrations, also observed in the copolymer. The PHB-*b*-PCL spectrum shows a strong presence of PCL in the copolymer structure indicated by the more intense bands related to the  $\text{CH}_2$  bond at  $2900\text{ cm}^{-1}$  (stretching) and  $1380\text{ cm}^{-1}$  (rocking). The intense bands attributed to ester C–O bonds indicate the maintenance of the chemical structure. As expected, there was no absorption in the region of  $3500\text{ cm}^{-1}$  representing the OH absorption region, whose absence indicates control of the hydrolysis reaction, favoring the transesterification reaction.



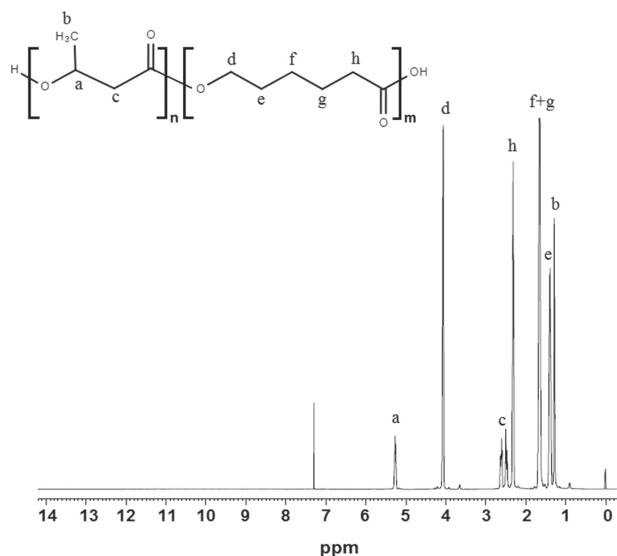
**Figure 1.** FTIR spectra (ATR) of PHB, PCL and PHB-*b*-PCL.

Figure 2 shows the  $^{13}\text{C}$  NMR spectrum of PHB-*b*-PCL with chemical shift assignments for each carbon. The spectrum indicates the presence of both segments, PCL and PHB, with predominance of PCL, indicated by the relatively greater intensity of the corresponding carbonyl. This demonstrates that PCL segments were introduced into the PHB chains by transesterification.



**Figure 2.**  $^{13}\text{C}$  NMR spectrum (125 MHz,  $\text{CDCl}_3$ ) of PHB-*b*-PCL.

The mixed structure of the copolymer was confirmed by Figure 3, which shows the  $^1\text{H}$  NMR spectrum of the copolymer with the corresponding assignments. The signals attributed to PHB segments were observed at  $\delta$  1.27 (doublet), 2.45-2.63 (multiplet) and 5.24-5.28 (quartet). All the expected peaks of individual constituents could be found in the copolymer, suggesting block copolymer formation. There is a direct proportional correlation between the integrated area of the peaks and the number of protons that generated these peaks, allowing the composition quantification of PHB and PCL content. A ratio of PHB to PCL of 1:2 was found, indicating that a considerable amount of PHB has not reacted during the transesterification and was removed by the purification procedure.



**Figure 3.**  $^1\text{H}$  NMR spectrum (500 MHz,  $\text{CDCl}_3$ ) of PHB-*b*-PCL.

The solubility tests of PHB-*b*-PCL showed a mixed character indicating the copolymer formation. PHB is insoluble in all solvents tested except  $\text{CHCl}_3$ , in which it was soluble after heating. Conversely, PCL was soluble in all solvents but MeOH, in which it was partially soluble. The product was soluble in  $\text{CHCl}_3$ , DCM and DCE, partially soluble in THF and non-soluble in MeOH; therefore, comparatively more soluble in organic solvents than PHB and less than PCL. Figure 4 shows the different solubility behavior of PHB and PHB-*b*-PCL dissolved in DCE.

Interactions between the polymer and solvents were analyzed by comparing the solvent position with respect to the soluble region in the three-dimensional space for the given polymer, the Hansen parameters, divided into three-component to account for the dispersion,  $\delta_d$ , the polar interactions,  $\delta_p$ , and hydrogen bonding,  $\delta_h$ . Hansen

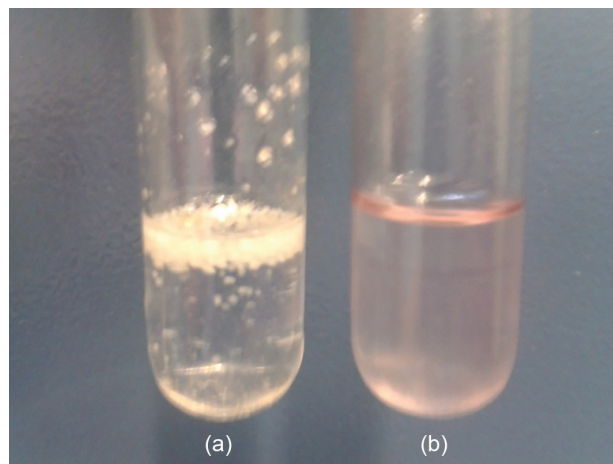


**Figure 4.** Solubility comparison between (a) PHB and (b) PHB-*b*-PCL dissolved in DCE.

solubility parameters were calculated for the copolymer based on the group contribution method applied on partial solubility parameters for the proportions of PHB and PCL.<sup>25</sup> Table 1 shows the copolymer Hansen solubility components and total solubility parameter closer to PCL values than that of PHB.

**Table 1.** Hansen parameters for homopolymers and copolymer at 25 °C

Polymer	$\delta_d / \text{MPa}^{1/2}$	$\delta_p / \text{MPa}^{1/2}$	$\delta_h / \text{MPa}^{1/2}$	$\delta / \text{MPa}^{1/2}$
PHB	15.5 <sup>a</sup>	9.0 <sup>a</sup>	8.6 <sup>a</sup>	19.9 <sup>a</sup>
PCL	17.0 <sup>b</sup>	4.8 <sup>b</sup>	8.3 <sup>b</sup>	19.5 <sup>b</sup>
PHB- <i>b</i> -PCL	16.5	6.2	8.4	19.5

<sup>a</sup>Obtained from Terada and Marchessault publication;<sup>26</sup> <sup>b</sup>obtained from the Hansen publication.<sup>27</sup>  $\delta_d$ : Hansen dispersion component;  $\delta_p$ : Hansen polar interactions component;  $\delta_h$ : Hansen hydrogen bonding component;  $\delta$ : solubility parameter; PHB: poly(3-hydroxybutyrate); PCL: poly( $\epsilon$ -caprolactone); PHB-*b*-PCL: poly(3-hydroxybutyrate-*b*- $\epsilon$ -caprolactone).

Table 2 shows values for the Hansen parameters for the solvents used. This explains why the copolymer is more soluble in the solvents tested; however, it is not enough to make an accurate solubility evaluation, since the solubility parameter concept is applicable only to amorphous polymer. The crystalline shell of the PHB granule could cause PHB to be insoluble in most solvents at room temperature.<sup>26</sup>

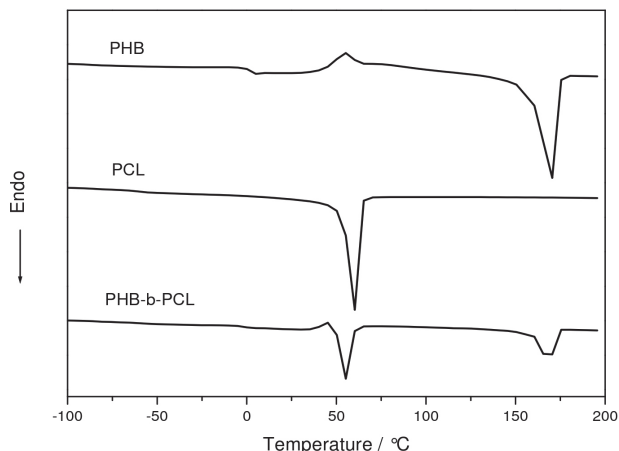
DSC curves are shown in Figure 5. The DSC curve of PHB-*b*-PCL showed crystallization at 44.9 °C followed by melting at 57.2 °C, and then a further melting at 169.1 °C, corresponding to the melting of crystals formed by PCL and PHB segments, respectively. The main thermal parameters obtained from DSC analysis are summarized in Table 3.

The cold crystallization of PHB segments in the copolymer occurred at a lower temperature than that

**Table 2.** Hansen parameters for solvents at 25 °C<sup>a</sup>

Solvent	$\delta_d$ / MPa <sup>1/2</sup>	$\delta_p$ / MPa <sup>1/2</sup>	$\delta_h$ / MPa <sup>1/2</sup>	$\delta$ / MPa <sup>1/2</sup>
1,2-Dichloroethane (DCE)	19.0	7.4	4.1	20.8
Dichloromethane (DCM)	18.2	6.3	6.1	20.2
Chloroform (CHCl <sub>3</sub> )	17.8	3.1	5.7	18.9
Methanol (MeOH)	15.1	12.3	22.3	29.6
Tetrahydrofuran (THF)	16.8	5.7	8.0	19.5

<sup>a</sup>Obtained from the Hansen publication.<sup>27</sup>  $\delta_d$ : Hansen dispersion component;  $\delta_p$ : Hansen polar interactions component;  $\delta_h$ : Hansen hydrogen bonding component;  $\delta$ : solubility parameter.

**Figure 5.** DSC curves of PHB, PCL and copolymer PHB-*b*-PCL.

observed for PHB, due to the probable partial miscibility with PCL segments. There was also a reduction in the melting temperatures of crystallites in relation to the homopolymers, confirming the effect of mutual disturbance of the PCL and PHB segments, which make it difficult to bend the chains to form larger and more perfect crystallites.

PHB and PCL homopolymers have high degree of crystallinity, 66.5 and 45.6%, respectively. The percentages of crystallinity due to PHB and PCL segments in the copolymer were 13.5 and 22.7%, respectively. The degrees of crystallinity ( $X_c$ ) of PCL and PHB segments in homopolymers and copolymer were determined from the melting enthalpy according to equation 1.

$$X_{c,i} = \frac{\Delta H_m}{\Delta H_m^0 w_i} \quad (1)$$

**Table 3.** Thermal parameters of homopolymers and copolymer

Polymer	$T_g$ / °C	$T_c$ / °C	$T_m$ / °C		$\Delta H_m$ / (J g <sup>-1</sup> )		$X_c$ / %	
			PCL	PHB	PCL	PHB	PCL	PHB
PHB	2.7	55.3	–	170.4	–	96.9	–	66.5
PCL	–60.8	NO	60.4	–	61.5	–	45.6	–
PHB- <i>b</i> -PCL	–59.0 / –1.1	44.9	57.2	169.1	30.6	19.7	22.7	13.5

$T_g$ : glass transition temperature;  $T_c$ : crystallization temperature;  $T_m$ : melting temperature;  $\Delta H_m$ : melting enthalpy of the sample;  $X_c$ : degree of crystallinity; PHB: poly(3-hydroxybutyrate); PCL: poly( $\epsilon$ -caprolactone); PHB-*b*-PCL: poly(3-hydroxybutyrate-*b*- $\epsilon$ -caprolactone); NO: non-observed.

where  $\Delta H_m$  is the melting enthalpy of the sample and  $\Delta H_m^0$  is the melting enthalpy of the 100% crystalline polymer. Reference values for  $\Delta H_m^0$  of 146 J g<sup>-1</sup><sup>21</sup> was adopted for PHB, and 136 J g<sup>-1</sup><sup>28</sup> for PCL.  $w_i$  is the weight fraction of the corresponding block in the mixture. In the copolymer, the PCL and PHB fractions were estimated by <sup>1</sup>H NMR spectrometry.

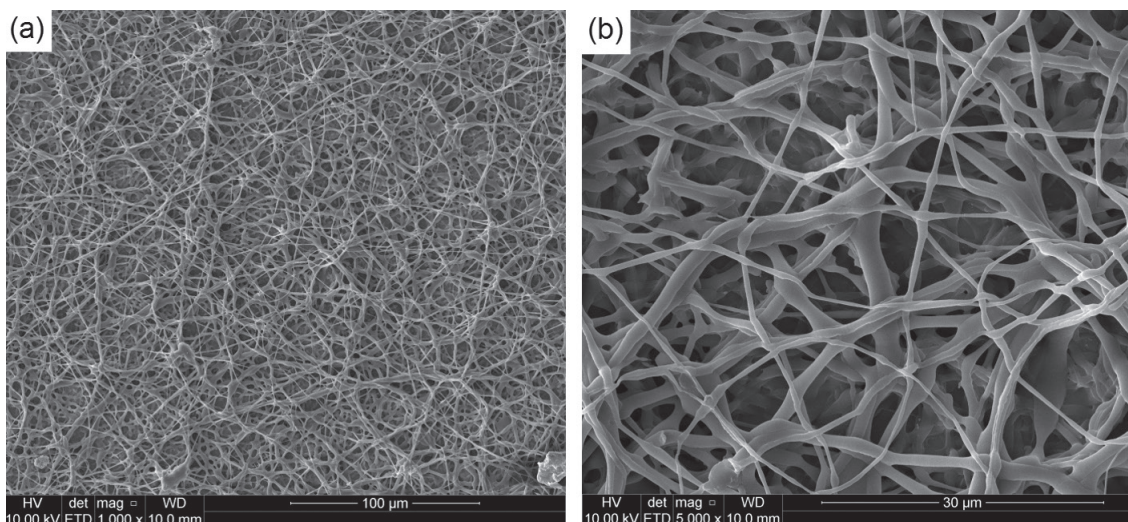
The results indicate a decrease of the crystalline fraction of the copolymer as well as a reduction of the crystalline melting temperatures for both PCL and PHB phases, as would be expected for a copolymer.

Two PHB-*b*-PCL solutions, 20 and 25 wt.%, were successfully submitted to electrospinning with fiber formation as observed by SEM. Figure 6 shows the morphology of the fibrous structure obtained from the 20 wt.% solution, whereby the main electrospinning conditions were set as feeding rate of 1 mL h<sup>-1</sup>, voltage of 12 kV and 15 cm of working distance. Some fibers are observed to be bound and stuck to each other, generating a network of interconnected fibers, which presented a diameter range from 450 to 1100 nm. These features are considered to be a consequence of delayed evaporation of the solvent, when the ejected solution reaches the collector, however, within no sufficient time to evaporate, and the formed fiber jets piled up on each other before solidification. Instant solidification in the collector is crucial during the electrospinning to ensure the fibers cylindrical morphology and to preserve the porous structure.<sup>29</sup> The variation in the fiber diameter could be attributed to the jet instability during the process.

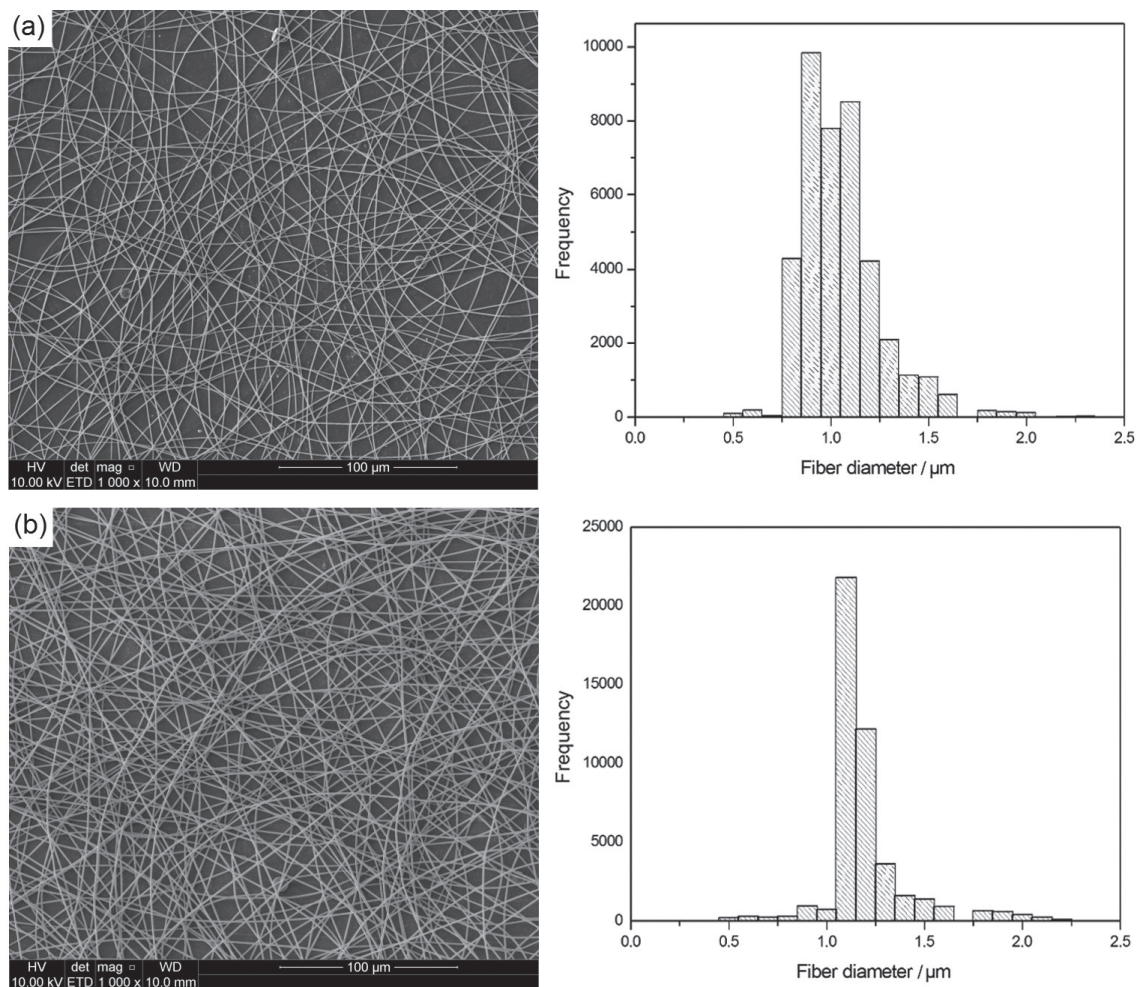
Figure 7 presents the morphology and the fiber diameter distributions in the mats prepared from the 25 wt.% solution.

Figure 7a shows the results under the previous operating condition set for the 20 wt.% solution, while in Figure 7b, the same 25 wt.% solution was submitted to almost the same

conditions, except that the feeding rate was incremented to  $1.2 \text{ mL h}^{-1}$ . However, both electrospun mats from the 25 wt.% solution presented similar uniform morphology, but a larger



**Figure 6.** SEM images for 20 wt.% solution concentration under operating parameters  $1 \text{ mL h}^{-1}$ , 12 kV, 15 cm with magnification of (a) 1,000 $\times$ ; (b) 5,000 $\times$ .



**Figure 7.** SEM images and fiber diameter distribution histogram for 25 wt.% solution concentration under different operating parameters: (a)  $1 \text{ mL h}^{-1}$ , 12 kV, 15 cm and (b)  $1.2 \text{ mL h}^{-1}$ , 12 kV, 15 cm.

variation in fiber diameters was detected in the first one, the flow rate of which was lower, while the second presented a smaller quantity of droplets, greater dimensional stability and the fiber diameter increased slightly. The fibers collected at the flow rate of 1.0 mL h<sup>-1</sup> have average diameter between 900 and 1100 nm as compared to the 1100 and 1200 nm observed at the higher flow rate of 1.2 mL h<sup>-1</sup>; additionally, the diameter distribution became narrower. Increasing the solution concentration resulted in more homogeneous fibers with few beads. When the concentration of the solution is high, more uniform fibers are formed because of the higher viscosity resistance.<sup>30</sup>

The SEM images display significant empty spaces between the fibers, due to the random orientation of the deposition of the material on the collector. Actually, the mats are essentially formed by voids. For applications in tissue engineering, these pores enhance the fluid absorption and facilitate cell incorporation and perfusion.<sup>31,32</sup> In addition, due to the small fiber diameters, the specific surface area is high, allowing better adsorption of proteins and cell membrane receptors.<sup>13,33</sup>

## Conclusions

In this work, PHB-*b*-PCL was successfully synthesized by transesterification of PHB, as hard segments, and PCL, as soft segments, using reactive extrusion. The PHB-*b*-PCL presented predominance of PCL segments and reduced crystallinity, facilitating its application in biomaterials. Smooth and uniform fibers with average diameters between 900 and 1200 nm were obtained by electrospinning. More uniform fibers were acquired when more concentrated solution was electrospun. In addition to the solution concentration, other parameters, such as applied voltage and flow rate, also affected the formation and size of the fibers. PHB-*b*-PCL sub micrometric fiber membranes here prepared are potential candidates for producing scaffolds for cell growth, indicating a promising biodegradable material to be made available in the future in the field of biomedicine.

## Acknowledgments

This study was supported by the Brazilian Coordination for the Improvement of Higher Education Personnel (CAPES, finance code 001) and by the Brazilian Council for Scientific and Technological Development (CNPq).

## References

1. Cao, K.; Liu, Y.; Olkhov, A. A.; Siracusa, V.; Iordanskii, A. L.; *Drug Delivery Transl. Res.* **2018**, *8*, 291.

2. Castellano, D.; Sanchis, A.; Blanes, M.; Perez Del Caz, M. D.; Ruiz-Sauri, A.; Piquer-Gil, M.; Pelacho, B.; Marco, B.; Garcia, N.; Ontoria-Oviedo, I.; Cambra, V.; Prosper, F.; Sepulveda, P.; *J. Tissue Eng. Regen. Med.* **2018**, *12*, e983.
3. Jiang, Y.; Jia, G.; Zhicai, X.; Kyoung-Jin, S.; Insook, H.; Jung-Chul, K.; Inn-Kyu, K.; Jian, S.; *J. Tissue Eng. Regen. Med.* **2015**, *9*, 1027.
4. Sombatmankhong, K.; Sanchavanakit, N.; Pavasant, P.; Supaphol, P.; *Polymer* **2007**, *48*, 1419.
5. Salvatore, L.; Carofiglio, V. E.; Stufano, P.; Bonfrate, V.; Calo, E.; Scarlino, S.; Nitti, P.; Centrone, D.; Cascione, M.; Leporatti, S.; Sannino, A.; Demitri, C.; Madaghiele, M.; *J. Healthcare Eng.* **2018**, *2018*, 13.
6. Moncada, J.; Matallana, L. G.; Cardona, C. A.; *Ind. Eng. Chem. Res.* **2013**, *52*, 4132.
7. Petrasovits, L. A.; Purnell, M. P.; Nielsen, L. K.; Brumbley, S. M.; *Plant Biotechnol. J.* **2007**, *5*, 162.
8. Petrasovits, L. A.; Zhao, L.; McQualter, R. B.; Snell, K. D.; Somleva, M. N.; Patterson, N. A.; Nielsen, L. K.; Brumbley, S. M.; *Plant Biotechnol. J.* **2012**, *10*, 569.
9. Silva, L. F.; Taciro, M. K.; Ramos, M. E. M.; Carter, J. M.; Pradella, J. G. C.; Gomez, J. G. C.; *J. Ind. Microbiol. Biotechnol.* **2004**, *31*, 245.
10. Yu, J.; Stahl, H.; *Bioresour. Technol.* **2008**, *99*, 8042.
11. Alicata, R.; Barbuzzi, T.; Giuffrida, M.; Ballistreri, A.; *Rapid Commun. Mass Spectrom.* **2006**, *20*, 568.
12. Marega, C.; Marigo, A.; *J. Appl. Polym. Sci.* **2015**, *132*, 42265.
13. Karahaliloğlu, Z.; Demirbilek, M.; Şam, M.; Erol-Demirbilek, M.; Sağlam, N.; Denkbaş, E. B.; *J. Appl. Polym. Sci.* **2013**, *128*, 1904.
14. Ublekov, F.; Budurova, D.; Staneva, M.; Natova, M.; Penchev, H.; *Mater. Lett.* **2018**, *218*, 353.
15. Ghavimi, S. A. A.; Ebrahimzadeh, M. H.; Solati-Hashjin, M.; Osman, N. A. A.; *J. Biomed. Mater. Res., Part A* **2015**, *103*, 2482.
16. Woodruff, M. A.; Hutmacher, D. W.; *Prog. Polym. Sci.* **2010**, *35*, 1217.
17. Lim, J. S.; Ki, C. S.; Kim, J. W.; Lee, K. G.; Kang, S. W.; Kweon, H. Y.; Park, Y. H.; *Biopolymers* **2012**, *97*, 265.
18. Chen, C.; Fei, B.; Peng, S.; Wu, H.; Zhuang, Y.; Chen, X.; Dong, L.; Feng, Z.; *J. Polym. Sci., Part B: Polym. Phys.* **2002**, *40*, 1893.
19. Kim, B. O.; Woo, S. I.; *Polym. Bull.* **1998**, *41*, 707.
20. Impallomeni, G.; Giuffrida, M.; Barbuzzi, T.; Musumarra, G.; Ballistreri, A.; *Biomacromolecules* **2002**, *3*, 835.
21. Garcia-Garcia, D.; Rayón, E.; Carbonell-Verdu, A.; Lopez-Martinez, J.; Balart, R.; *Eur. Polym. J.* **2017**, *86*, 41.
22. Jean-Marie, R.; Ramani, N.; Philippe, D.; *Macromol. Mater. Eng.* **2008**, *293*, 447.
23. Kampeerapappun, P.; *J. Appl. Polym. Sci.* **2016**, *133*, 43273.

24. Hotaling, N. A.; Bharti, K.; Kriel, H.; Simon Jr., C. G.; *Biomaterials* **2015**, *61*, 327.
25. Schenderlein, S.; Lück, M.; Müller, B. W.; *Int. J. Pharm.* **2004**, *286*, 19.
26. Terada, M.; Marchessault, R. H.; *Int. J. Biol. Macromol.* **1999**, *25*, 207.
27. Hansen, C. M.; *Hansen Solubility Parameters: A User's Handbook*, 2<sup>nd</sup> ed.; CRC Press: Boca Raton, USA, 2007.
28. Wu, L.; Chen, S.; Li, Z.; Xu, K.; Chen, G.-Q.; *Polym. Int.* **2008**, *57*, 939.
29. Fang, J.; Wang, H.; Niu, H.; Lin, T.; Wang, X.; *J. Appl. Polym. Sci.* **2010**, *118*, 2553.
30. Bhardwaj, N.; Kundu, S. C.; *Biotechnol. Adv.* **2010**, *28*, 325.
31. Aghdam, R. M.; Najarian, S.; Shakhesi, S.; Khanlari, S.; Shaabani, K.; Sharifi, S.; *J. Appl. Polym. Sci.* **2012**, *124*, 123.
32. Norouzi, M.; Boroujeni, S. M.; Omidvarkordshouli, N.; Soleimani, M.; *Adv. Healthcare Mater.* **2015**, *4*, 1114.
33. Agarwal, S.; Wendorff, J. H.; Greiner, A.; *Adv. Mater.* **2009**, *21*, 3343.

Submitted: April 21, 2020

Published online: September 11, 2020

